

Electroless copper deposition as a seed layer on TiSiN barrier

Y. C. Ee^{a)} and Z. Chen

School of Materials Engineering, Nanyang Technological University, Singapore 639798

S. Xu

Plasma Sources and Applications Centre, NIE, Nanyang Technological University, Singapore 639798

L. Chan, K. H. See, and S. B. Law

Chartered Semiconductor Manufacturing, 60 Woodlands Industrial Park D, Street 2, Singapore 738406

(Received 3 November 2003; accepted 15 March 2004; published 23 July 2004)

Electroless deposition of copper as a seeding technology has received considerable attention in back-end-of-line device fabrication. This work explores the effects of plasma processing parameters such as argon gas flow rate and nitrogen plasma treatment time on the properties of electrolessly plated Cu on TiSiN barrier layers. The barrier film was produced by a low-frequency inductively coupled plasma process. The properties of deposited electroless copper are characterized by x-ray diffraction, four-point resistivity probe, atomic force microscopy, and field emission scanning electron microscope. The required palladium activation time is greatly reduced on TiSiN compared to TiN. In both cases there exists a preferred (111) crystal orientation in Cu film and the intensity ratio of $I(111)/I(200)$ is very close. The Cu grain size is within the range of 23–34 nm for 84 nm thick film. It is found that argon gas flow rate does not have a significant effect on the resistivity of electroless copper film on TiSiN. However, increasing nitrogen plasma treatment time reduces the resistivity of copper film. The roughness of plated Cu layer largely follows the one of the underlying TiSiN. Good surface coverage of electroless Cu seed layer on TiSiN has been achieved in our experiment. © 2004 American Vacuum Society. [DOI: 10.1116/1.1738658]

I. INTRODUCTION

As the semiconductor industry moves toward deep sub-100 nm gates with much reduced interconnect line pitch, copper interconnect emerges as an important candidate. The need for copper as a low resistivity metal which lowers the RC signal delay of interconnect lines is well understood.^{1,2} However, the successful incorporation of copper into submicron devices requires an improved diffusion barrier. The requirements for such a barrier layer include conformal step coverage for high aspect ratio features, compatibility with low- k dielectric materials as well as low resistivity to maintain device performance. Recently, TiSiN as a diffusion barrier has been shown to possess the required electrical, chemical, structural, and thermal properties and has been successfully integrated in sub-130 nm copper/low- k semiconductor device technology nodes.³ Various research groups have grown Ti–Si–N films by physical vapor deposition, metal-organic chemical-vapor deposition, and metal-organic atomic layer deposition techniques, and documented their resulting performance as copper diffusion barriers.^{3–8} However, to the knowledge of the authors, there has been little work on the deposition of electroless copper seed layer on TiSiN barrier film, which is a necessary step for the subsequent electroplating process in the back end of line microelectronics.

In our work, TiSiN was formed by low frequency inductively coupled plasma (ICP) process and the properties of the film was reported elsewhere.⁹ ICP featuring high ion densities and low plasma potentials have advantages in generating

large-area and large volume plasma for fabrication and processing of unique materials in the back end of line microelectronics. This article discusses the effect of plasma process parameters on electrolessly deposited copper film. The surface coverage, surface morphology, film resistivity, uniformity, surface roughness, crystal orientation, and copper grain size are reported.

II. EXPERIMENT

50 nm TiSi film was fabricated by depositing a layer of Ti on silicon wafers first, followed by rapid thermal annealing at 750 °C (RTA1) and 850 °C (RTA2). High density nitrogen implantation into TiSi film was conducted in a low frequency inductively coupled plasma reactor. The chamber was evacuated to 1×10^{-4} Torr (base pressure) before the processing gases were introduced. Low frequency ~ 0.5 MHz has been applied for the inductive plasma production. Argon, hydrogen, and nitrogen gases were used in our investigation. The nitrogen plasma treatment time was chosen to be 30 and 60 min and the argon flow rate varied from 10 to 30 sccm. Details of the processing parameters are shown in Table I. The total gas pressure was maintained at 2×10^{-2} Torr, the substrate temperature was between 200 and 300 °C, and the plasma power was 2 kw. TiN barrier film prepared by chemical vapor deposition was used as a reference material.

Before electroless Cu plating, samples went through standard SC1 and SC2 cleaning processes. Catalyzation was carried out by immersing the samples into the activating solution, which contains HF, HCl, and PdCl₂. After the activation, electroless copper deposition was immediately carried out at temperature between 60–62 °C. The deposition

^{a)}Electronic mail: PA8898695@ntu.edu.sg

TABLE I. ICPs process parameters at different argon flow rate and nitrogen treatment time.

Sample	Ar Flow rate (sccm)	N ₂ treatment time (min)
I	10	30
K	20	30
M	30	30
J	10	60
L	20	60
N	30	60

time was kept at 8 min for all samples. The electroless copper bath consists mainly of copper sulphate CuSO₄ (which acts as a oxidant and provides the source of cupric ions), ethylene diamine tetraacetic acid (EDTA, as a complexing agent), and formaldehyde, HCHO (reductant). The pH level was maintained at 12.8.

Field emission scanning electron microscope was used to observe surface coverage and surface morphology of the electroless copper film. The resistivity of the as-deposited electroless copper film was measured using the ResMap™ four-point probe system. Transmission electron microscope was employed to observe the grain size. The thickness of the electrolessly plated copper film was separately measured by TEM observation of the cross-section, and depth-profile by time-of-flight secondary ion mass spectroscopy. The difference in copper film thickness between the two measurements is within 1.5%. Atomic force microscope was employed to assess the roughness of the film. The crystallinity, texture and grain size of the deposited film were determined by x-ray diffraction (XRD) using a Shimadzu™ XRD 6000 diffractometer.

The mean grain size d_{mean} of electrolessly plated copper was estimated using the (111) peak broadening according to Scherrer's equation:¹⁰

$$d_{\text{mean}} = \frac{0.94 \times \lambda_{\text{Cu}}}{W_{\text{eff}} \times \cos 2\theta}, \quad (1)$$

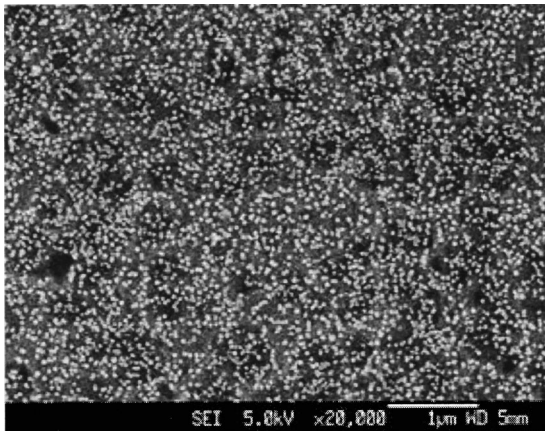


FIG. 1. Distribution of palladium seeds on TiSiN after 1 min activation. Nitrogen plasma treatment time is 60 min.

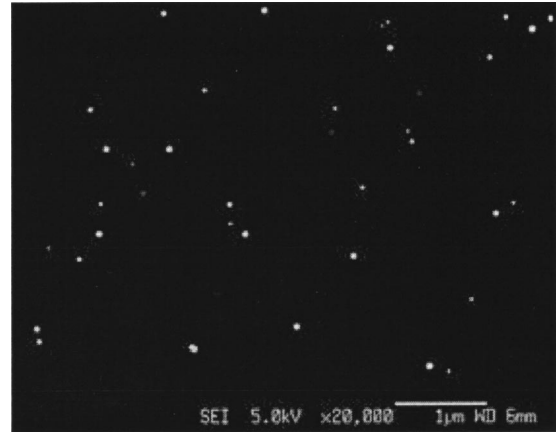


FIG. 2. Distribution of palladium seeds on TiN after 1 min activation.

where λ_{Cu} =wavelength of Cu $K\alpha=0.1542$ nm, W_{eff} =effective full width at half maximum, and 2θ =diffraction angle.

The effective full width W_{eff} was determined from the Gaussian distribution function of the (111) peak, curve-fitted from experimental measurement. Instrumental broadening was calibrated before applying Eq. (1) for the grain size calculation. Analysis based on the data obtained in the current study shows the error in d_{mean} is between 7% and 11% due to curve-fitting error.

III. RESULTS AND DISCUSSION

A blanket Si wafer with TiSiN/TiSi/Si film stack was used for the Pd activation and subsequent electroless Cu plating. The required activation time on TiSiN was found to be 1 min or less as compared to 3 min on TiN. This time is determined by the amount and distribution of Pd seeds that will successfully induce copper plating.¹¹⁻¹³ As shown in Figs. 1–3, the density of Pd for 1 min activation on TiSiN is much higher than the one on TiN for as long as 3 min. For the TiN surface, 1 min activation could not produce an effective surface for electroless Cu plating (Fig. 2) since there are too few Pd seeds. There are two possible reasons for the difference in Pd

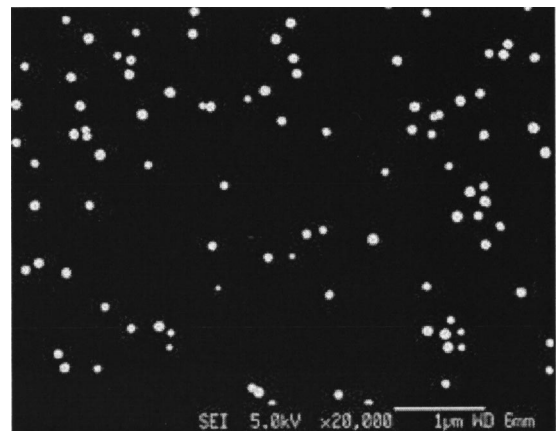


FIG. 3. Distribution of palladium seeds on TiN after 3 min activation.

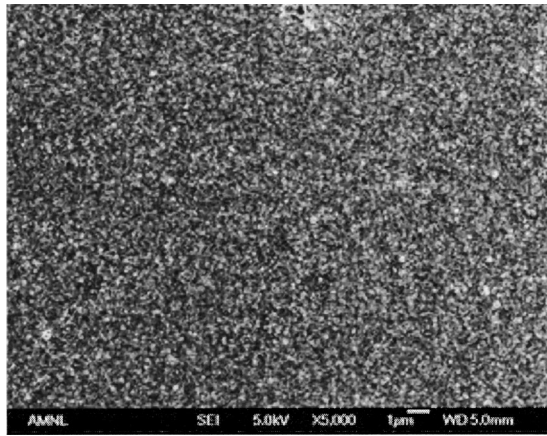


FIG. 4. Surface coverage of electrolessly plated copper on TiSiN film after 8 min deposition.

seed distribution. One possibility is the Pd/substrate interfacial energy between the barrier films. The activation energy for Pd nucleation is lower on the TiSiN surface, which leads to higher nucleation rate. Another contributing factor could be the damage on the TiSiN surface in the form of dangling bonds due to plasma implantation; free electrons are available to speed up the reduction of Pd from Pd⁺⁺. It is interesting to observe such a drastic change in Pd activation behavior on the two barrier films. Detailed work on understanding the mechanisms is still on-going.

Figure 4 shows that an average thickness of ~85 nm electroless copper deposited on TiSiN film with 100% surface coverage. These samples were subjected to 1 min Pd activation. Good surface coverage is due to coalescence of the copper islands on the densely populated Pd seeds on TiSiN surface.¹⁴ Figure 5 shows an average thickness of ~85 nm electroless copper deposited on TiN film with good surface coverage, the sample was subjected to 3 min Pd activation for the reason mentioned before. Comparing the two cases, shorter Pd activation time is required on TiSiN in order to achieve a good surface coverage of electroless copper.

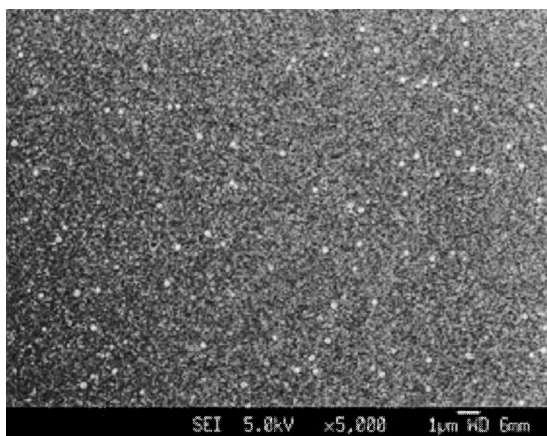


FIG. 5. Surface coverage of electrolessly plated copper on TiN film after 8 min deposition.

TABLE II. Mean grain size and surface roughness of electroless copper on TiSiN.

Sample	Mean grain size (nm)	Average surface roughness (nm)	Resistivity ($\mu\Omega$ cm)	Error associate with resistivity measurement
I	23.2	30.4	9.5	± 0.67
K	24.6	25.9	9.3	± 0.77
M	23.7	28.9	9.9	± 0.40
J	28.0	36.2	7.1	± 0.45
L	32.7	32.2	7.8	± 0.67
N	34.1	23.9	7.7	± 0.83

For a fixed nitrogen plasma treatment time, sheet resistance of electroless copper film was measured as a function of argon gas flow rate. Sheet resistance of the copper layer is found to be less than 1.2 ohms/sq in all cases. Besides that, changes in argon gas flow rate do not show a significant effect on resistivity of electroless copper layer. A mean value of 9.6 $\mu\Omega$ cm is obtained in those samples (I,K,M) as shown in Table II. These samples have undergone different argon gas flow rate at fixed 30 min nitrogen plasma treatment. In addition, this result is further confirmed by comparing samples J, L, and N, which have undergone different argon gas flow rate at fixed 1 h nitrogen plasma treatment. The mean resistivity value of 7.6 $\mu\Omega$ cm is obtained. This gives rise to the following conclusion: argon gas flow rate does not have a significant effect on the resistivity of electroless copper film on TiSiN.

Nitrogen plasma treatment time was found to affect the resistivity of electroless copper seed layer. Current work shows that there is a 20% reduction in copper film resistivity as nitrogen plasma treatment time increases from 30 to 60 min. The resistivity change could be explained by the Cu grain size difference. Table II shows that, regardless of the Ar flow rate, Cu grain size in samples J, L, and N (60 min N₂ treatment time), is larger than the one in samples I, K, and M (30 min N₂ treatment time). Comparing Fig. 1, which shows

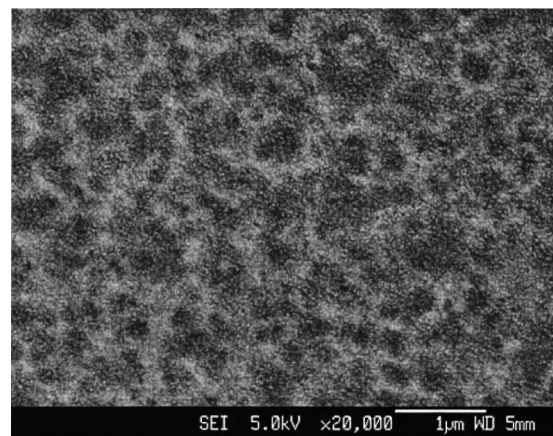


FIG. 6. Distribution of palladium seeds on TiSiN which has been subjected to 30 min nitrogen treatment. Palladium seeds are smaller and more densely populated compared with 60 min plasma treatment as shown in Fig. 1.

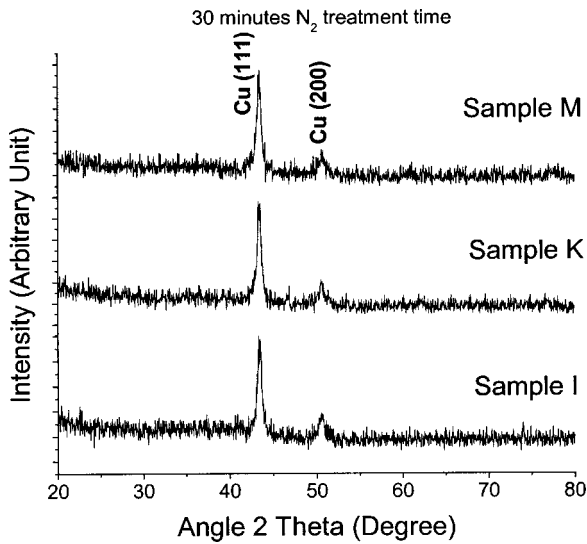


FIG. 7. XRD measurement for different argon gas flow rate. Nitrogen plasma treatment time is 30 min.

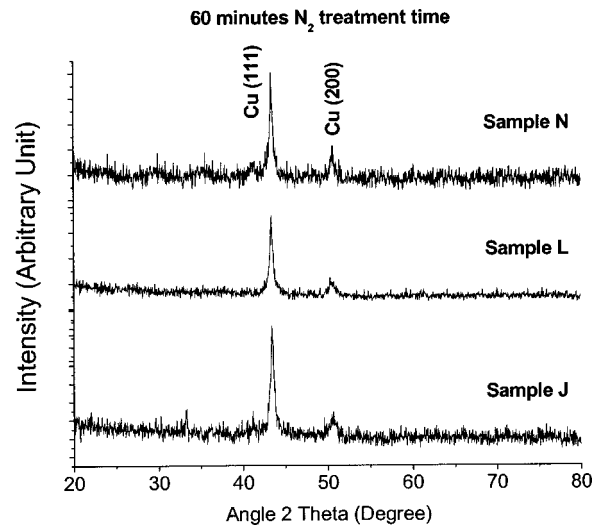


FIG. 8. XRD measurement for different argon gas flow rate. Nitrogen plasma treatment time is 60 min.

the palladium seed distribution on sample N, and Fig. 6, which displays the one from sample M, it is clear that the palladium nuclei in sample N are larger and more sparsely populated. The sparsely distributed palladium seeds will lead to larger copper grain size, and thus lower resistivity. Further discussion on the relationship between the grain size and the film resistivity will be provided below. Here we are interested in why a longer plasma treatment time leads to larger and less densely distributed Pd. It is understood that longer treatment time will lead to higher surface energy due to the damage caused by plasma bombardment. Pd nucleation rate ought to be higher on the surface of higher energy. To explain the observation made in our experiment (that in samples with longer treatment time the Pd seed density is

lower), requires a full record of Pd nucleation and growth. Since the current work only compares the Pd distribution at a fixed activation time, a conclusive explanation might not be attainable. We speculate that due to the higher surface energy, the required incubation time for nucleation is shorter. Therefore although the initial nucleation density is higher, there is enough time for the Pd seeds to ripen after nucleation. Work is still on-going in the authors' laboratory to investigate the Pd nucleation and growth behavior on the barrier film.

Copper grain orientation was characterized by XRD patterns shown in Figs. 7 and 8. This work finds that there is a preferred (111) crystal orientation in all the prepared samples. As for randomly oriented powdered Cu samples,

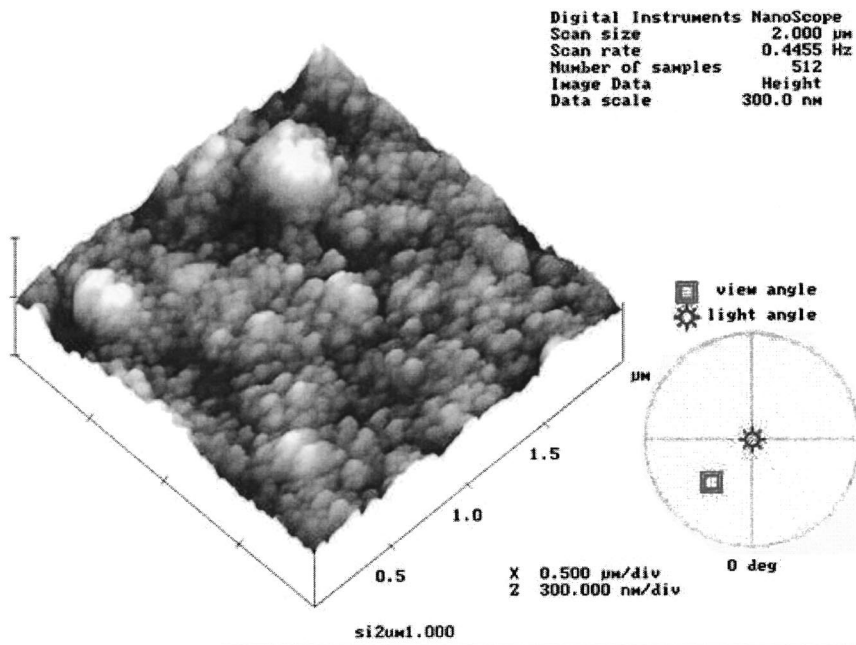


FIG. 9. Three-dimensional stereographical AFM images of electroless copper on TiSiN layer.

$I_{(111)}/I_{(200)} = 2.17$. This factor increases to about 2.7 in all the samples obtained in this work. This implies that copper grains orientation is independent of the barrier surface condition as a result of changing the argon gas flow rate and nitrogen treatment time.

The texture of electroless copper is important as the Cu film is used as seed layer for Cu electroplating in ultra large scale integration. The plated Cu film will adopt the texture of the seed layer (epitaxial effect) and the (111) texture is preferred for better electromigration performance.¹⁵ In addition, large Cu grains in the seed layer will produce large Cu grains during electroplating process, and thus near bamboo structure in the interconnect becomes more possible. Bamboo structure is known to enhance the electromigration resistance and increase the lifetime of interconnects.

In addition, Cu (111) planes have the lowest surface energy among all Cu planes. The relationship between the mechanical properties and the crystal structure of copper film is influenced by the texture. For face-center-cubic copper, the stronger the preferred orientation with (111) planes, the greater the tensile strength. The strain up to the elastic fracture will increase when (111) texture becomes stronger.

When electroless copper deposits on the TiSiN which has undergone different argon flow rates and 30 min nitrogen plasma treatment (samples I, K, and M), the mean grain size of electroless copper is about 23 nm as shown in Table II. There is an increase in copper grain size when TiSiN has undergone 60 min nitrogen plasma treatment (samples J, L, and N). The mean copper grain size increases from 28 to 34 nm as the argon flow rate changes from 10 to 30 sccm. This shows that larger copper grain size can be obtained by depositing copper seed layer onto the TiSiN barrier layer which has been subjected to a higher argon flow rate and longer nitrogen plasma treatment. As discussed previously, this process conditions may lead to sparsely distributed Pd seeds on TiSiN. As a result, larger copper grains can be produced. As reported by Harper *et al.*,¹⁶ the larger the copper grain size, the lower the resistivity of copper thin film. This is believed by the authors to be related to grain boundary scattering effect. Our experiment observed the similar trend: The copper film that was deposited on TiSiN subjected to 60 min nitrogen treatment has a larger grain size of 34 nm and a corresponding resistivity value $\sim 7.57 \mu\Omega \text{ cm}$, while the one with 30 min nitrogen treatment has a smaller copper grain size of 23 nm and a resistivity $\sim 9.6 \mu\Omega \text{ cm}$.

Root mean square surface roughness of electroless copper deposited on TiSiN was measured by atomic force microscopy (AFM). Figure 9 shows one of the surface profile of plated copper film. Prior to activation and electroless copper

deposition, surface roughness of TiSiN is within the range of 18–23 nm. After the deposition, surface roughness of plated Cu seed layer is within the range of 23–36 nm. The slight increase in surface roughness is largely caused by the Pd islands on the TiSiN surface which lead to rapid localized electroless copper growth on these nuclei at the initial stage of copper plating, leading to the increase in roughness after plating.

IV. CONCLUSION

The properties of electroless copper seed layers deposited on TiSiN barrier films have been studied. With TiSiN as a barrier layer, the palladium activation time is greatly reduced compared to TiN. Good surface coverage of the electroless copper seed layer on TiSiN is obtainable. The resistivity of electroless copper seed layer is affected by nitrogen plasma treatment time. Larger copper grains and (111) texture can be achieved when the TiSiN layer is subjected to longer nitrogen plasma treatment. The results of the current work indicate that electroless copper can be successfully used as a seed layer on TiSiN barrier film.

¹National Technology Roadmap for Semiconductors (Semiconductor Industry Association, San Jose, CA, 2001).

²D. S. Gardner, J. D. Meindl, and K. C. Saraswat, *IEEE Trans. Electron Devices* **34**, 3 (1987).

³C. Marcadal, M. Eizenberg, A. Yoon, and L. Chen, *J. Electrochem. Soc.* **149**, C52 (2002).

⁴Eric Eisenbraun and Allan Upham, *J. Vac. Sci. Technol. B* **4**, 18 (2000).

⁵Edward Norton, Jr. and Carmela C. Amato-Wierda, *Surf. Coat. Technol.* **148**, 251 (2001).

⁶J. S. Reid, X. Sun, E. Kolawa, and M.-A. Nicolet, *IEEE Electron Device Lett.* **15**, 298 (1994).

⁷J. S. Min, H. S. Park, and S. W. Kang, *Appl. Phys. Lett.* **75**, 1521 (1999).

⁸J. S. Min, Y. W. Son, W. G. Kang, S. S. Chun, and S. W. Kang, *Jpn. J. Appl. Phys., Part 1* **37**, 4999 (1998).

⁹Y. C. Ee, S. Xu, Z. Chen, L. Chan, Alex K. H. See, S. B. Law, Z. L. Tskadze, P. Rutkevich, K. Y. Zeng, and L. Shen, *International Conference on Materials for Advanced Technologies* (Institute of Materials Research and Engineering, Singapore, 2003).

¹⁰Ken. M. Takahashi, *Proceedings of the IEEE 1999 International Interconnect Technology Conference* (Institute of Electrical and Electronics Engineers, San Francisco, 1999), pp. 281–283.

¹¹W. L. Goh, K. T. Tan, M. S. Tse, and K. Y. Liu, *Int. J. Mod. Phys. B* **16**, 197 (2002).

¹²J. C. Patterson, C. Ni Dheasuna, J. Barrett, T. R. Spalding, M. O'Reilly, X. Jiang, and G. M. Crean, *Appl. Surf. Sci.* **91**, 124 (1995).

¹³P. P. Lau, C. C. Wong, L. Chan, A. See, S. B. Law, and K. T. Tan (unpublished).

¹⁴Yosi Y. Shacham-Diamand, *Electrochem. Solid-State Lett.* **3**, 279 (2000).

¹⁵C. Ryu, K. W. Kwon, A. S. K. Loke, H. Lee, T. Nogami, V. Dubin, R. A. Kavari, G. Ray, and S. Wong, *IEEE Trans. Electron Devices* **46**, 1113 (1999).

¹⁶J. M. E. Harper, C. Cabral, Jr., P. C. Andricacos, L. Gignac, I. C. Noyan, K. P. Rodbell, and C. K. Hu, *J. Appl. Phys.* **86**, 2516 (1999).